Efficient calculation of two-dimensional periodic and waveguide acoustic Green's functions

K. V. Horoshenkov[a]
School of Engineering, University of Bradford, Bradford BD7 1DP, United Kingdom

Simon N. Chandler-Wilde[b]
Department of Mathematical Sciences, Brunel Unversity, Uxbridge UB8 3PH, United Kingdom

New representations and efficient calculation methods are derived for the problem of propagation from an infinite regularly spaced array of coherent line sources above a homogeneous impedance plane, and for the Green's function for sound propagation in the canyon formed by two infinitely high, parallel rigid or sound soft walls and an impedance ground surface. The infinite sum of source contributions is replaced by a finite sum and the remainder is expressed as a Laplace-type integral. A pole subtraction technique is used to remove poles in the integrand which lie near the path of integration, obtaining a smooth integrand, more suitable for numerical integration, and a specific numerical integration method is proposed. Numerical experiments show highly accurate results across the frequency spectrum for a range of ground surface types. It is expected that the methods proposed will prove useful in boundary element modeling of noise propagation in canyon streets and in ducts, and for problems of scattering by periodic surfaces. © *2002 Acoustical Society of America.* [DOI: 10.1121/1.1460920]

I. INTRODUCTION

In the last 10 to 20 years the popularity of numerical modeling of sound propagation has received a substantial impetus as a result of the continuous increase in computer speed and storage capacity. The boundary element method has emerged as a powerful numerical technique for modeling sound propagation in the presence of multiple scattering and diffracting objects with complex shapes. In outdoor acoustics two-dimensional versions of the boundary element method have been exploited to predict the efficiency of noise barriers (e.g., Refs. 1–3) and the effect of building façades.[4] In principle, the method is not limited by the extent of the acoustic region of interest. However, restrictions are imposed by the size of the available computer memory and execution times can be unacceptably slow if the discretization of larger boundaries at shorter wavelengths is required.

The number of boundary elements required can be reduced drastically by using a Green's function in the boundary integral equation formulation which incorporates analytically many of the physical boundary conditions of the problem. In this paper we propose methods for computation of the Green's function for sound propagation in a two-dimensional canyon/waveguide, occupying the part of the Oxy plane, $0<x<h$, $y>0$, with rigid or sound soft boundary conditions on $x=0$ and $x=h$ for $y>0$ and an impedance boundary condition on $y=0$, $0<x<h$. It is envisaged that this Green's function will prove useful for the efficient investigation by boundary element simulations of noise propagation in city streets. In this application the infinitely high walls at $x=0$ and $x=h$ would represent high rise building

facades and the impedance boundary condition at $y=0$ a reflecting or sound absorbing road surface. Boundary element discretization would only be required for additional structures, e.g., balconies and building features, sound absorbing treatments to building elements, noise barriers, etc. The actual finite height of building facades could be modeled accurately by imposing an absorbing boundary condition (requiring boundary element discretization) on sections of the walls at $x=0$ and $x=h$, starting at the heights where the buildings finish. The point of using the canyon/waveguide Green's function is that, rather than discretizing the whole of the physical boundary, only those parts of the boundary which are perturbations from the boundary conditions for the Green's function need be discretized, leading to much smaller storage and computational requirements. Use of a two-dimensional Green's function implies that the geometry must be a two-dimensional one, invariant in the horizontal z direction. For a completely 2D problem the sound sources must also be invariant in the z direction, so that the sources of sound are coherent line sources. The applicability of 2D boundary element models can, however, be extended to more general sound sources by partial Fourier transform techniques. These are discussed, for example, in Refs. 2 and 3, and predictions of outdoor sound propagation are made in Ref. 2 for point and incoherent line sources of sound using a 2D boundary element code. There has been considerable recent interest in making predictions of noise levels, using mathematical and experimental models, for the type of urban configuration described in this paragraph—see, e.g., Refs. 4–8. In particular, work by Tang[8] illustrates that the acoustic field near a finitely high building facade at a low receiver position can be predicted accurately using a model which assumes that the facade is infinitely high, so that the technique proposed above to model finitely high facades accu-

[a])Electronic mail: k.horoshenkov@bradford.ac.uk
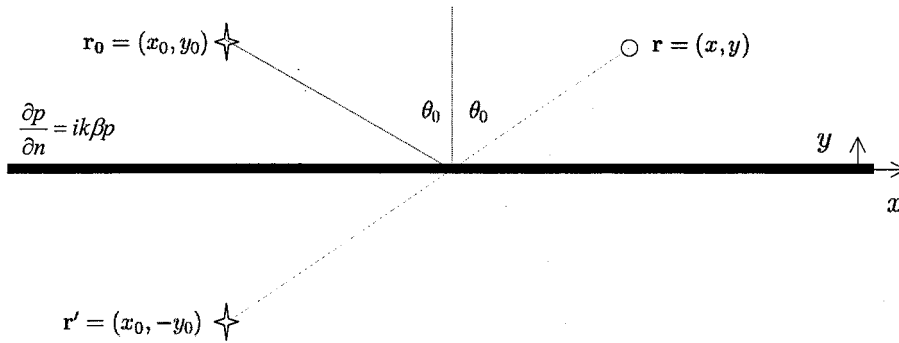[b])Electronic mail: simon.chandler-wilde@brunel.ac.uk

FIG. 1. Sound propagation above an impedance plane.

rately may be unnecessary. Tang's results are supported by close agreement between his theory and scale model experiments.[8]

Computing the canyon/waveguide Green's function requires calculation of the combined effect of the multiple reflections in the vertical rigid or sound soft walls at $x=0$ and $x=h$. This leads to an initial study of computation of the field due to an infinite array of periodically spaced point sources above a flat impedance boundary. The field due to such a periodic array of sources, extending to infinity in both directions, is usually termed the periodic Green's function. This function is utilized widely in the solution by integral equation methods of problems of acoustic and electromagnetic scattering by structures which are periodic in one dimension only. It is usual to utilize, in the numerical solution of such problems, the *free field periodic Green's function*, the solution to the calculation of the field due to an infinite periodic source array in free space, and there is a large literature on the computation of this function, reviewed recently in Ref. 9. In Secs. III and IV we discuss the computation of what may be termed the two-dimensional periodic Green's function for propagation above an impedance plane. The efficient calculation of this periodic Green's function appears not to have been discussed previously, although its use (and the use of other half-plane periodic Green's functions) in place of the free field periodic Green's function has been recommended recently for problems of scattering by one-dimensional periodic surfaces.[10,11] In particular, use of the impedance periodic Green's function in place of the free field function leads to integral equation formulations which are well-defined for all periods of the scattering surface. As is well known and discussed in Sec. III, the free field periodic Green's function is undefined for a sequence of values of the periodicity.

The method described for computing the impedance periodic Green's function, proposed in the thesis of the first author,[12] is to compute a finite number of the source contributions explicitly and represent the contributions from the remaining (infinite number of) source contributions as a single Laplace-type integral. This technique, with just a single source contribution computed explicitly, has been proposed for the much simpler free field periodic Green's function in Ref. 13 (and see Refs. 14, 15, and 9). The analysis presented here derives, for the first time, integral representations for the infinite sum of source contributions for the im-

pedance case. It is also shown, adapting methods for the case of a single source above an impedance boundary,[16] how parts of the integral, corresponding to poles of the integrand lying near the path of integration, can be evaluated explicitly in terms of the complementary error function, leaving a much smaller and smoother integrand to evaluate numerically. Finally, an explicit numerical integration scheme is proposed and its error analyzed, and it is shown how to select the number of source contributions to be computed explicitly so as to ensure high accuracy of calculation for the integral terms using only a 22-point quadrature rule. This attention to efficient evaluation is essential for the successful use of this Green's function in boundary element calculations. The accuracy and efficiency of the calculation method is illustrated by comparison with an alternative solution to the problem using normal mode decomposition.

II. THE GREEN'S FUNCTION FOR SOUND PROPAGATION ABOVE AN IMPEDANCE BOUNDARY

Consider the fundamental situation in which a monofrequency line source ($e^{-i\omega t}$ time dependence) is elevated above a flat boundary with normalized surface admittance β. Let $G_\beta(\mathbf{r}, \mathbf{r}_0)$ denote the acoustic pressure at $\mathbf{r}=(x,y)$ when the source is at $\mathbf{r}_0=(x_0, y_0)$. We note that $\beta=0$ if the boundary is rigid, while Re $\beta>0$ if the boundary is an energy-absorbing surface. In the case $\beta=0$ the sound field can be found, as the combination of a direct wave and a wave reflected by the surface (Fig. 1), to be

$$G_0(\mathbf{r}, \mathbf{r}_0) = -\frac{i}{4}H_0^{(1)}(k|\mathbf{r}_0 - \mathbf{r}|) - \frac{i}{4}H_0^{(1)}(k|\mathbf{r}_0 - \mathbf{r}'|), \quad (1)$$

where $\mathbf{r}'=(x_0, -y_0)$ is the position vector of the image of the source in the plane $y=0$, and $H_0^{(1)}$ is the Hankel function of the first kind of order zero.

In the more general case when $\beta\neq0$, the total field G_β can be written as

$$G_\beta(\mathbf{r}, \mathbf{r}_0) = G_0(\mathbf{r}, \mathbf{r}_0) + P_\beta(\mathbf{r}, \mathbf{r}_0), \quad (2)$$

where $P_\beta(\mathbf{r}, \mathbf{r}_0)$ is a perturbation term, accounting for the effect of nonzero admittance. Clearly $P_\beta=0$ if $\beta=0$. To determine the perturbation term P_β, for Re $\beta>0$, it is necessary to solve the Helmholtz equation
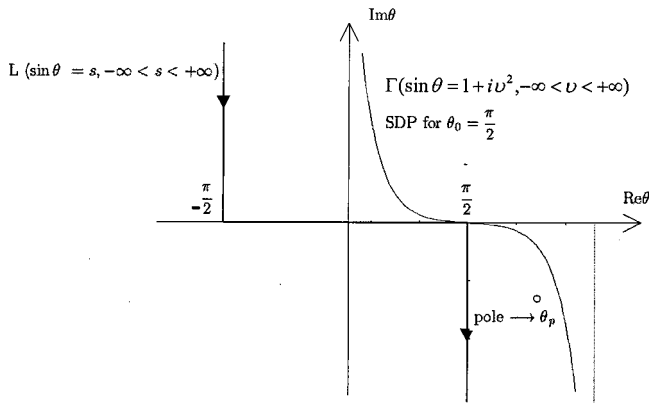
$$(\Delta + k^2)P_\beta = 0, \quad (3)$$

FIG. 2. The transformation of the integration path.

with the impedance boundary condition on $y=0$,

$$\frac{\partial}{\partial y}P_\beta(\mathbf{r},\mathbf{r}_0)+ik\beta P_\beta(\mathbf{r},\mathbf{r}_0)$$

$$=-ik\beta G_0(\mathbf{r},\mathbf{r}_0)=-\frac{k\beta}{2}H_0^{(1)}(k\sqrt{(x-x_0)^2+y_0^2}). \quad (4)$$

This can be accomplished by Fourier transform methods, as discussed, for example, in Ref. 16. The solution to (3) and (4) which also satisfies the Sommerfeld radiation condition,

$$\lim_{r\to\infty}r^{1/2}\left(\frac{\partial P_\beta(\mathbf{r},\mathbf{r}_0)}{\partial r}-ikP_\beta(\mathbf{r},\mathbf{r}_0)\right)=0, \quad (5)$$

is[16]

$$P_\beta(\mathbf{r},\mathbf{r}_0)=\frac{i\beta}{2\pi}\int_{-\infty}^{+\infty}\frac{e^{i\eta_+\sqrt{1-s^2}}}{\sqrt{1-s^2}(\sqrt{1-s^2}+\beta)}e^{-is|\xi_-|}ds, \quad (6)$$

where $\xi_-=k(x-x_0)$, $\eta_+=k(y+y_0)$, and the square root is taken with $\mathrm{Re}(\sqrt{1-s^2})\geq0$ and $\mathrm{Im}(\sqrt{1-s^2})\geq0$.

The representation (6) for $P_\beta(\mathbf{r},\mathbf{r}_0)$ is not suitable for evaluation by numerical integration as the integrand becomes increasingly oscillatory as $k|\mathbf{r}-\mathbf{r}_0|\to\infty$. A standard first step to a more suitable representation is to substitute $s=\sin\theta$. This change of variable transforms expression (6) into

$$P_\beta(\mathbf{r},\mathbf{r}_0)=\frac{i\beta}{2\pi}\int_L\frac{e^{i(\eta_+\cos\theta+|\xi_-|\sin\theta)}}{\cos\theta+\beta}d\theta. \quad (7)$$

Here L is the path of integration from $(-\pi/2+i\infty)$ $\to-\pi/2\to\pi/2\to(\pi/2-i\infty)$ which is shown in Fig. 2. The integrand has an infinite number of simple poles which occur at

$$\theta=\pm\theta_p+2\pi n, \quad n\in\mathbb{Z}, \quad (8)$$

where θ_p denotes the unique solution of $\cos\theta+\beta=0$ in $\pi/2$ $<\mathrm{Re}\,\theta<\pi$. The point θ_p lies above or below the real axis, depending on whether $\mathrm{Im}\,\beta>0$ or $\mathrm{Im}\,\beta<0$, respectively.

In Ref. 16, starting from Eq. (7), representations for P_β are derived which can be evaluated accurately and efficiently by Gauss–Laguerre quadrature rules. The method employed is to deform the path of integration to the steepest descent path, which connects $-\pi/2+i\infty$ to $\pi/2-i\infty$, passing

through $\theta=\theta_0$, where θ_0 is the angle of incidence as shown in Fig. 1. This path is given by $\cos(\theta-\theta_0)=1+iv^2$, $-\infty<v<\infty$. Then a pole subtraction technique is employed to smooth the behavior of the integrand on this path.

The methods proposed in Sec. III will make use of this representation, but a further representation for P_β will also be required. To develop this expression the choice is made to deform the path of integration to what is the steepest descent path in the case that the angle of incidence is $\theta_0=\pi/2$. This transformed path of integration Γ connects $i\infty$ to $(\pi-i\infty)$, cutting the real axis at $\theta=\pi/2$, and is defined by

$$\sin\theta=1+iv^2, \quad v\in\mathbb{R}, \quad (9)$$

with $0<\mathrm{Re}\,\theta<\pi/2$ for $v<0$, $\pi/2<\mathrm{Re}\,\theta<\pi$ for $v>0$, so that $\cos\theta=-v\sqrt{v^2-2i}$, with $\mathrm{Re}\,\sqrt{v^2-2i}>0$. The path Γ and the direction of integration as v increases from $-\infty$ to $+\infty$ are shown in Fig. 2. Making the deformation of the path of integration we obtain that

$$P_\beta^{(L)}=P_\beta^{(\Gamma)}+P_s, \quad (10)$$

where $P_\beta^{(\Gamma)}$ is the integral (7) with the path of integration changed from L to Γ and P_s is the contribution accounting for the residue at the pole θ_p, the only one which can be crossed in the deformation. Explicitly, where $\sqrt{1-\beta^2}$ denotes the square root with positive real part,

$$P_s=\begin{cases}\beta\dfrac{e^{-i\eta_+\beta}}{\sqrt{1-\beta^2}}e^{i|\xi_-|\sqrt{1-\beta^2}}\\[2mm]\quad\text{if }\mathrm{Im}\,\beta<0\;\text{ and }\mathrm{Re}\,\sqrt{1-\beta^2}>1,\\[2mm]\dfrac{\beta}{2}\dfrac{e^{-i\eta_+\beta}}{\sqrt{1-\beta^2}}e^{i|\xi_-|\sqrt{1-\beta^2}}\\[2mm]\quad\text{if }\mathrm{Im}\,\beta<0\;\text{ and }\mathrm{Re}\,\sqrt{1-\beta^2}=1,\\[2mm]0\quad\text{otherwise.}\end{cases} \quad (11)$$

Physically, this term is a surface wave which decays exponentially with height above the surface.

The first term on the right-hand side of Eq. (10) can be represented, via the parametrization (9), as the integral

$$P_\beta^{(\Gamma)}=\frac{\beta e^{i|\xi_-|}}{\pi}\int_{-\infty}^{+\infty}\frac{e^{-i\eta_+\sqrt{v^2-2i}}}{\sqrt{v^2-2i}(\beta-v\sqrt{v^2-2i})}e^{-|\xi_-|v^2}dv. \quad (12)$$

Splitting the range of integration in (12) and changing the sign of the variable of integration in the second integral, it is seen that, defining $w=v\sqrt{v^2-2i}$,

$$P_\beta^{(\Gamma)}=\frac{\beta e^{i|\xi_-|}}{\pi}\left[\int_0^\infty\frac{e^{-i\eta_+v\sqrt{v^2-2i}}}{\sqrt{v^2-2i}(\beta-v\sqrt{v^2-2i})}e^{-|\xi_-|v^2}dv\right.$$

$$\left.+\int_0^\infty\frac{e^{i\eta_+v\sqrt{v^2-2i}}}{\sqrt{v^2-2i}(\beta+v\sqrt{v^2-2i})}e^{-|\xi_-|v^2}dv\right]$$

$$=\frac{2\beta e^{i|\xi_-|}}{\pi}\int_0^\infty\frac{\beta\cos(\eta_+w)-iw\sin(\eta_+w)}{\sqrt{v^2-2i}(\beta^2-w^2)}e^{-|\xi_-|v^2}dv. \quad (13)$$

K. V. Horoshenkov and S. N. Chandler-Wilde: Waveguide Green's functions

To finish this section, a similar representation for the total field from a line monopole placed above the impedance surface is obtained. The total field is given as

$$G_\beta(\mathbf{r},\mathbf{r}_0) = G_0(\mathbf{r},\mathbf{r}_0) + P_\beta^{(\Gamma)} + P_s. \tag{14}$$

Further, in terms of the variables ξ_- and $\eta_\pm$, where $\eta_- = k(y - y_0)$, it holds that

$$G_0(\mathbf{r},\mathbf{r}_0) = -\frac{i}{4}\{H_0^{(1)}(\sqrt{\xi_-^2 + \eta_+^2}) + H_0^{(1)}(\sqrt{\xi_-^2 + \eta_-^2})\}. \tag{15}$$

Using a representation for the Hankel function as a Laplace-type integral (Ref. 17 formulas 2.13.52 and 2.13.60), the function G_0 can be represented in a similar form to (13), as

$$G_0(\mathbf{r},\mathbf{r}_0) = -\frac{e^{i|\xi_-|}}{\pi}\int_0^\infty \frac{\cos(\eta_+ w) + \cos(\eta_- w)}{\sqrt{v^2 - 2i}} e^{-|\xi_-|v^2} dv. \tag{16}$$

Combining (13), (14), and (16), it is seen that

$$G_\beta(\mathbf{r},\mathbf{r}_0) = \frac{e^{i|\xi_-|}}{\pi}\int_0^\infty \left[\frac{w^2(\cos(\eta_+ w) + \cos(\eta_- w)) - 2i\beta w \sin(\eta_+ w)}{\sqrt{v^2 - 2i}(\beta^2 - w^2)} + \frac{\beta^2(\cos(\eta_+ w) - \cos(\eta_- w))}{\sqrt{v^2 - 2i}(\beta^2 - w^2)}\right] e^{-|\xi_-|v^2} dv + P_s. \tag{17}$$

III. PROPAGATION OF SOUND FROM AN INFINITE NUMBER OF PERIODICALLY SPACED SOURCES

Consider the problem of an infinite number of equidistantly spaced sources elevated at the same height above an impedance plane as shown in Fig. 3, at positions $\mathbf{r}_l = (x_l, y_0)$, $l = 0, 1, \ldots$, where $x_l = x_0 + 2hl$ and $2h$ is the distance between adjacent sources. Suppose that the sources have the same unit strength but allow the possibility that there is a phase shift of $2H\alpha$ between adjacent sources, where $H = kh$ and α is some fixed real number. Using the same notation as in Sec. II, the resultant field at an arbitrary observation point $\mathbf{r} = (x,y)$ can be written as the superposition of the contributions from all the sources as

$$G_\beta^P(\mathbf{r},\mathbf{r}_0;\alpha) = \sum_{l=0}^\infty e^{-2il\alpha H} G_\beta(\mathbf{r},\mathbf{r}_l). \tag{18}$$

Provided Re $\beta > 0$ (the boundary is energy absorbing) and the source and receiver remain close to the ground surface, $G_\beta(\mathbf{r},\mathbf{r}_l)$ decays, as the distance between source and receiver increases, at a rate which is faster than in free-field conditions. A full far-field asymptotic expansion for G_β, quantifying this behavior, is given in Ref. 18. The leading asymptotic behavior can also be seen directly from (17). Note first that P_s decays exponentially as $|x - x_0| \to \infty$. The integral in (17) has the form

$$\int_0^\infty Q(v^2) e^{-|\xi_-|v^2} dv = \frac{1}{2}\int_0^\infty s^{-1/2} Q(s) e^{-|\xi_-|s} ds,$$
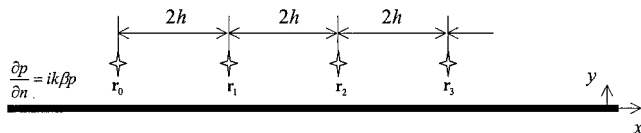
FIG. 3. The set of periodically spaced sources above the impedance boundary.

where the function Q has the asymptotic behavior $Q(s) \sim as$ as $s \to 0$, where

$$a = \frac{\sqrt{-2i}}{2\beta^2}[4 - 4i\beta\eta_+ + \beta^2(\eta_+^2 - \eta_-^2)].$$

It follows from Watson's lemma (e.g., Ref. 19 p. 263) that

$$G_\beta(\mathbf{r},\mathbf{r}_l) = O(|x - x_l|^{-3/2})$$

as $|x - x_l| \to \infty$ with y and y_0 fixed. This rate of decay ensures that the infinite series (18) is absolutely convergent, which in turn ensures that the validity of the interchange of integration and infinite summation in the manipulations below is valid, at least for the case Re $\beta > 0$.

The summation corresponding to (18) in the free-field case is studied extensively in the literature: this work has been clearly reviewed by Linton.[9] This summation is

$$G_f^P(\mathbf{r},\mathbf{r}_0;\alpha) = \sum_{l=0}^\infty e^{-2il\alpha H} G_f(\mathbf{r},\mathbf{r}_l), \tag{19}$$

where G_f is the standard free-field Green's function, defined by $G_f(\mathbf{r},\mathbf{r}_l) = -(i/4) H_0^{(1)}(k|\mathbf{r} - \mathbf{r}_l|)$. In contrast to (18), in the case Re $\beta > 0$, the series (19) is only conditionally convergent, since the Hankel function has the asymptotic behavior $H_0^{(1)}(t) \sim \sqrt{2/\pi t} e^{i(t - \pi/4)}$ as $t \to \infty$. Indeed, if $\alpha = 0$, (19) is divergent to infinity if the wavelength divides the period, i.e., if H is an integer multiple of π. More generally, for an arbitrary value of α, the series (19) diverges if $H(1 - \alpha)$ is an integer multiple of π. The same restriction, that the series is only conditionally convergent, or divergent in the case that $H(1 - \alpha)$ is a multiple of π, carries over to (18) in the case $\beta = 0$. Physically, this divergence corresponds to cases where the contributions from far source points are all in phase, and combine to give an infinite pressure field at the receiver position.

The first N terms can be extracted from the sum (18) to

be evaluated explicitly, using the efficient calculation method proposed in Ref. 16. The remaining sum, from N to infinity, can be expressed as a single infinite integral by replacing G_β by its integral representation (17), reversing the order of summation and integration, and finally evaluating the summation under the integral sign, which is now a geometric series. Provided N is chosen large enough so that $x_N > x$, the resulting expression is

$$G_\beta^P(\mathbf{r},\mathbf{r}_0;\alpha) = \sum_{l=0}^{N-1} e^{-2il\alpha H} G_\beta(\mathbf{r},\mathbf{r}_l)$$
$$+ \frac{2e^{i(\xi_N - 2N\alpha H)}}{\pi} \int_0^\infty f(v^2) e^{-\xi_N v^2} dv + P_s^P,$$

$$(20)$$

where $\xi_N = k(x_N - x)$, the function f is defined implicitly by

$$f(v^2) = \frac{w^2 \cos(\eta_0 w)\cos(\eta w) - \beta^2 \sin(\eta_0 w)\sin(\eta w) - i\beta w \sin(\eta_+ w)}{\sqrt{v^2 - 2i}(\beta^2 - w^2)(1 - e^{-2H(v^2 - i(1-\alpha))})}, \tag{21}$$

with $\eta_0 = ky_0$ and $\eta = ky$, and P_s^P is the sum of the surface wave contributions, given by

$$P_s^P = \begin{cases} \beta \dfrac{e^{-i\eta_+ \beta} e^{i(\xi_N \sqrt{1-\beta^2} - 2N\alpha H)}}{\sqrt{1-\beta^2}} [1 - e^{2iH(\sqrt{1-\beta^2} - \alpha)}]^{-1} \\ \quad \text{if } \operatorname{Im}\beta < 0 \text{ and } \operatorname{Re}\sqrt{1-\beta^2} > 1, \\[2mm] \dfrac{\beta}{2} \dfrac{e^{-i\eta_+ \beta} e^{i(\xi_N \sqrt{1-\beta^2} - 2N\alpha H)}}{\sqrt{1-\beta^2}} [1 - e^{2iH(\sqrt{1-\beta^2} - \alpha)}]^{-1} \\ \quad \text{if } \operatorname{Im}\beta < 0 \text{ and } \operatorname{Re}\sqrt{1-\beta^2} = 1, \\[2mm] 0 \quad \text{otherwise.} \end{cases}$$

$$(22)$$

A discussion of the choice of N in (20) follows in Sec. III B.

A. Pole subtraction

As mentioned already, in the representation (20) for $G_\beta^P(\mathbf{r},\mathbf{r}_0;\alpha)$ the contributions from the terms $G_\beta(\mathbf{r},\mathbf{r}_l)$ in the finite summation can be evaluated using the method proposed in Ref. 16. This method represents $G_\beta(\mathbf{r},\mathbf{r}_l)$ as the sum of an expression involving the complementary error function of complex argument and a Laplace-type integral which, as shown in Ref. 16, can be evaluated accurately and efficiently using a 22-point Gauss–Laguerre quadrature rule. To evaluate $G_\beta^P(\mathbf{r},\mathbf{r}_0;\alpha)$ using Eq. (20), it remains to consider the evaluation of the integral on the right-hand side of that equation, for which a similar integration scheme will be developed.

It is necessary first to examine the singularities of the function $f(z)$ and their proximity to the path of integration (the positive real axis). This is important because the accuracy of numerical integration methods is seriously affected if a singularity in the integrand lies on or near the integration path. It will become apparent that the only singularities which may lie close to the path of integration are poles. Further, a method of subtraction of the poles nearest to the positive real axis will be described leading to alternative representations of the integral in (20) as the sum of a Laplace-type integral and expressions involving the complementary

error function of complex argument. In these expressions, in contrast to the original integral in (20), the integrand is a smooth function for all values of β and H.

Substituting $t = \xi_N v^2$ in the integral in (20), this equation becomes

$$G_\beta^P(\mathbf{r},\mathbf{r}_0;\alpha) = \sum_{l=0}^{N-1} e^{-2il\alpha H} G_\beta(\mathbf{r},\mathbf{r}_l) + \frac{e^{i(\xi_N - 2N\alpha H)}}{\pi\sqrt{\xi_N}} I + P_s^P, \tag{23}$$

where

$$I = \int_0^\infty f(t/\xi_N) t^{-1/2} e^{-t} dt. \tag{24}$$

This integral can be approximated by Gaussian quadrature with weight function $t^{-1/2} e^{-t}$, in other words, by generalized Gauss–Laguerre quadrature,[20] and this will be accurate, using a rule with a small number of points, provided $f(t/\xi_N)$ is smooth as a function of t on the interval of integration, $0 \le t < \infty$. This will be the case provided $f(t/\xi_N)$ does not have singularities close to the positive real axis.

From (21), the function f is given explicitly by

$$f(z) = \frac{F(z)}{\sqrt{z-2i}(\beta^2 + 2iz - z^2)(1 - e^{-2H(z - i(1-\alpha))})}, \tag{25}$$

where

$$F(z) = z(z-2i)\cos(\eta_0\sqrt{z(z-2i)})\cos(\eta\sqrt{z(z-2i)})$$
$$- \beta^2 \sin(\eta_0\sqrt{z(z-2i)})\sin(\eta\sqrt{z(z-2i)})$$
$$- i\beta\sqrt{z(z-2i)}\sin(\eta_+\sqrt{z(z-2i)}). \tag{26}$$

The function F, the numerator in (25), is an entire function, i.e., is analytic in the whole complex plane. Provided the square root in (25) is chosen with $\operatorname{Re}\sqrt{z-2i} > 0$, $\sqrt{z-2i}$ is analytic in the half-plane $\operatorname{Im} z < 2$, which includes the positive real axis. The remaining singularities of f are poles at the points z which are the solutions of the equations

$$z^2 - 2iz - \beta^2 = 0 \tag{27}$$

and

$$1 - qe^{-2Hz} = 0, \tag{28}$$

where $q = e^{2iH(1-\alpha)}$.

The solutions of (27) are $z = i(1 \pm \sqrt{1-\beta^2})$. One of these solutions lies in the half-plane $\mathrm{Im}\, z \geqslant 1$. Choosing the square root so that $\mathrm{Re}\, \sqrt{1-\beta^2} \geqslant 0$, the other solution, in $\mathrm{Im}\, z \leqslant 1$, is

$$z_a = i(1 - \sqrt{1-\beta^2}) = i\beta^2/(1 + \sqrt{1-\beta^2}). \qquad (29)$$

Noting that $|z_a| \leqslant |\beta|^2$, it becomes clear that this root may lie on or arbitrarily close to the positive real axis, though $z_a \neq 0$ provided $\beta \neq 0$. In the numerical results reported in this paper, the effect of this pole will be ignored if $|\mathrm{Re}\, \sqrt{1-\beta^2}| \geqslant 0.75$ or $\mathrm{Im}\,(1 - \sqrt{1-\beta^2}) \geqslant 0.75$, in which case z_a lies at least distance 0.75 from the positive real axis. Otherwise the effect of this pole will be subtracted, i.e., the integral I will be rewritten as

$$I = \int_0^\infty g_a(t/\xi_N) t^{-1/2} e^{-t} dt + \epsilon_a \int_0^\infty \frac{t^{-1/2} e^{-t}}{t/\xi_N - z_a} dt, \qquad (30)$$

where

$$g_a(z) = f(z) - \frac{\epsilon_a}{z - z_a} \qquad (31)$$

and

$$\epsilon_a := \mathrm{Res}_{z=z_a} f(z)$$
$$= -\frac{F(z_a)}{2\sqrt{z_a - 2i}(z_a - i)(1 - e^{-2H(z_a - i(1-\alpha))})}, \qquad (32)$$

with

$$F(z_a) = \beta^2 [\cos(\eta_0 \beta)\cos(\eta\beta) - \sin(\eta_0 \beta)\sin(\eta\beta)$$
$$- i\sin(\eta_+ \beta)]. \qquad (33)$$

The point of the pole subtraction in (30) is that the second integral can be evaluated exactly. From Ref. 21, Eqs. (7.1.3) and (7.1.4), it follows, for arbitrary complex $z \neq 0$, that

$$\int_0^\infty \frac{t^{-1/2} e^{-t}}{t/\xi_N - z} dt = -i\pi \frac{\xi_N}{\sqrt{\xi_N z}} e^{-\sqrt{z\xi_N}} [\mathrm{erfc}(-i\sqrt{z\xi_N}) - \Psi(z)], \qquad (34)$$

where, if z is not on the positive real axis, then the square roots in (34) are to be taken with positive imaginary part. In Eq. (34), erfc is the complementary error function of complex argument, defined by $\mathrm{erfc}\, w = (2/\sqrt{\pi}) \int_w^\infty e^{-t^2} dt$, and

$$\Psi(z) = \begin{cases} 1, & z > 0, \\ 0, & \text{otherwise.} \end{cases} \qquad (35)$$

Note that $\Psi(z) = 1$ if and only if $\mathrm{Im}\, \beta < 0$ and $\mathrm{Re}\, \sqrt{1-\beta^2} = 1$, which is the same condition as selects the second alternative in Eq. (22).

The solutions of (28), which are the other poles of f, are

$$z = i\frac{\arg q + 2\pi n}{2H}, \quad n \in \mathbb{Z}, \qquad (36)$$

where $\arg q$ denotes the principal argument of q, in the range $-\pi < \arg q \leqslant \pi$. The closest of these poles to the positive real axis is that at

$$z_b = i\frac{\arg q}{2H}. \qquad (37)$$

The other poles have imaginary parts satisfying $|\mathrm{Im}\, z| \geqslant \pi/(2H)$, and so lie at least this distance from the real axis. In the numerical results shown below the pole at $z = z_b$ is subtracted if $0 < \arg q \leqslant \pi/4$, in which case $0 < |\mathrm{Im}\, z_b| \leqslant \pi/(8H)$. [If $\arg q = 0$, then the apparent singularity, at $z = z_b = 0$, is removable since $F(0) = 0$.] The same technique for removing the pole is utilized as has been described above for the pole at $z = z_a$, noting that

$$\epsilon_b := \mathrm{Res}_{z=z_b} f(z) = \frac{F(z_b)}{2\sqrt{z_b - 2i}(\beta^2 - z_b^2 + 2iz_b)H}. \qquad (38)$$

If only the pole at $z = z_b$ is to be subtracted, the resulting expression for the integral, Eq. (44), is similar to (30), but with $g_a(t/\xi_N)$ replaced by $g_b(t/\xi_N)$, where the function g_b is defined by

$$g_b(z) = f(z) - \frac{\epsilon_b}{z - z_b}. \qquad (39)$$

In the case that both the poles at z_a and z_b are to be subtracted, then $g_a(t/\xi_N)$ is replaced by $g_{ab}(t/\xi_N)$, where

$$g_{ab}(z) = f(z) - \frac{\epsilon_a}{z - z_a} - \frac{\epsilon_b}{z - z_b}. \qquad (40)$$

To sum up, the following expressions for the integral I are proposed for $\mathrm{Re}\, \beta > 0$, the different expressions below depending on whether the poles z_a and z_b are, or are not, "close" to the positive real axis, where, as mentioned above, it is proposed to treat z_a as lying close to the positive real axis if $\mathrm{Re}\, z_a > -0.75$ and $|\mathrm{Im}\, z_a| < 0.75$, i.e., if $\mathrm{Im}\,(1 - \sqrt{1-\beta^2}) > 0.75$ and $|\mathrm{Re}\, \sqrt{1-\beta^2}| < 0.75$, and z_b as lying close to the real axis if $|\mathrm{Im}\, z_b| < \pi/(8H)$, i.e., if $|\arg q| < \pi/4$. In each of the cases the integral to be calculated takes the form $\int_0^\infty g(t/\xi_N) t^{-1/2} e^{-t} dt$, for some function g. The pole subtraction carried out ensures that, in each case, the integrand $g(t/\xi_N)$ is bounded and analytic, as a function of t, in a neighborhood of the positive real axis, namely the strip $\mathrm{Re}\, t > -3\xi_N/4$, $|\mathrm{Im}\, t| \leqslant \min(\frac{3}{4}, \pi/(8H))\xi_N$. Thus it can be ensured that in each case singularities of the integrand do not lie closer than distance $\frac{3}{4}$ from the positive real axis by choosing N so that $\xi_N \geqslant \max(1, 6H/\pi)$. In other words, since $\xi_N = \xi_0 - \xi + 2HN$, where $\xi_0 = kx_0$ and $\xi = kx$, N is to be chosen in the range

$$N \geqslant \max\left(\frac{1}{2H}, \frac{3}{\pi}\right) - \frac{\xi_0 - \xi}{2H}. \qquad (41)$$

The four cases to be considered and the respective integral representations to be used for numerical evaluation are as follows. Recall that, in Eqs. (43)–(45), the square roots $\sqrt{z_a \xi_N}$ and $\sqrt{z_b \xi_N}$ are to be taken with argument in the range $[0, \pi)$.

I. Neither of the poles are close to the positive real axis (or $z_b = 0$ and z_a is not close to the positive real axis):

$$I = \int_0^\infty f(t/\xi_N) t^{-1/2} e^{-t} dt. \qquad (42)$$

II. The pole z_a is close to the positive real axis and either $z_b=0$ or z_b is not close to the real axis:

$$I = \int_0^\infty g_a(t/\xi_N) t^{-1/2} e^{-t} dt + \frac{i\epsilon_a \pi \xi_N}{\sqrt{z_a \xi_N}} e^{-z_a \xi_N}$$

$$\times [\mathrm{erfc}(-i\sqrt{z_a \xi_N}) - \Psi(z_a)]. \quad (43)$$

III. Only the pole z_b is close to the real axis (but $z_b \neq 0$):

$$I = \int_0^\infty g_b(t/\xi_N) t^{-1/2} e^{-t} dt + \frac{i\epsilon_b \pi \xi_N}{\sqrt{z_b \xi_N}} e^{-z_b \xi_N}$$

$$\times \mathrm{erfc}(-i\sqrt{z_b \xi_N}). \quad (44)$$

IV. Both the poles z_a and z_b are close to the positive real axis (but $z_b \neq 0$ and $z_a \neq z_b$):

$$I = \int_0^\infty g_{ab}(t/\xi_N) t^{-1/2} e^{-t} dt + i\pi \xi_N$$

$$\times \left[\frac{\epsilon_a}{\sqrt{z_a \xi_N}} e^{-z_a \xi_N} [\mathrm{erfc}(-i\sqrt{z_a \xi_N}) - \Psi(z_a)] \right.$$

$$\left. + \frac{\epsilon_b}{\sqrt{z_b \xi_N}} e^{-z_b \xi_N} \mathrm{erfc}(-i\sqrt{z_b \xi_N}) \right]. \quad (45)$$

The above formulas apply if $\mathrm{Re}\,\beta > 0$ (the boundary is energy absorbing). An important special case not covered above is that of a rigid boundary with $\beta = 0$. In this case, as noted earlier, the series (19) is divergent if $H(1-\alpha)$ is a multiple of π, in other words, if $q=1$. If $q \neq 1$, then it can be shown, via arguments similar to those used to derive the representation (20), that the summation (19) is (conditionally) convergent, and has the value given by (23) and (24), with the function f simplifying in this case to

$$f(z) = -\frac{\cos(\eta_0 \sqrt{z(z-2i)}) \cos(\eta \sqrt{z(z-2i)})}{\sqrt{z-2i}(1 - e^{-2H(z-i(1-\alpha))})}.$$

B. Numerical integration and choice of the parameter N

As indicated earlier, it is proposed to evaluate each of the integrals in Eqs. (42)–(45) by generalized Gauss–Laguerre quadrature. Let $x_{1,n}, x_{2,n}, \ldots, x_{n,n}$ denote the abscissae and $w_{1,n}, w_{2,n}, \ldots, w_{n,n}$ the weights of the n-point Gauss–Laguerre quadrature rule for the weight function $t^{-1/2} e^{-t}$. These weights and abscissae are tabulated for $n = 1, 2, \ldots, 15$ in Ref. 20 and for $n = 1, 2, 3$ in Ref. 16, or can be calculated using a standard subroutine library.[22] Let g denote one of the functions f, g_a, g_b, or g_{ab}. Then the numerical integration method employed will be to approximate

$$J := \int_0^\infty g(t/\xi_N) t^{-1/2} e^{-t} dt \approx J_{m,n} := \sum_{j=1}^m w_{j,n} g(x_{j,n}/\xi_N). \quad (46)$$

For $m = n$ the approximation, $J_{m,n}$, is the n-point Gauss–Laguerre rule approximation to the integral J. For $1 \le m$

$< n$, $J_{m,n}$ is an approximation to the Gauss–Laguerre rule obtained by neglecting the last $n - m$ weights and abscissae. Since the weights $w_{j,n}$ become extremely small for j and n large, $J_{m,n}$ can be just as accurate as $J_{n,n}$ while needing fewer terms in the summation (46) and thus being cheaper to evaluate.

The error in the numerical integration scheme proposed will now be examined. For brevity this error will be estimated only for the integral (42) in case I, where $g = f$ and z_a is at least distance $\pi/(8H)$ and z_b is at least distance 0.75 from the positive real axis. However, a similar analysis and nearly identical criteria for accuracy apply in the other three cases—cf. Ref. 16, Appendix B, and Ref. 23.

The error, $|J - J_{m,n}|$, in the numerical integration method has two components. One component arises from the neglect of the last $n - m$ weights and abscissae. The effect of this is equivalent to setting the integrand to zero beyond the mth abscissa, $x_{m,n}$. For this to be accurate it is necessary that the integrand $f(t/\xi_N) t^{-1/2} e^{-t}$ be small for $t > x_{m,n}$. To simplify the task of bounding f the assumption will be made that $|\beta| \le 1$, which range of β includes the values usually of interest in applications of the impedance boundary condition in outdoor sound propagation, where β is the relative surface impedance of the ground surface. Recalling that the case considered is that in which z_a and z_b are not close to the positive real axis, it then follows that, for $z \ge 0$,

$$|1 - e^{-2H(z-i(1-\alpha))}| \ge \frac{1}{\sqrt{2}}, \quad |\sqrt{z-2i}| \ge \sqrt{2},$$

$$|\beta^2 + 2iz - z^2| \ge \tfrac{3}{4},$$

and, where $\phi = |z(z-2i)|$,

$$|z(z-2i)/(\beta^2 + 2iz - z^2)| \le \frac{\phi}{\max(\tfrac{3}{4}, \phi - 1)} \le \frac{7}{3}.$$

Further,

$$|\cos(\eta_0 \sqrt{z(z-2i)})| \le e^{\eta_0 p(z)},$$

where $p(z) = |\mathrm{Im}\,\sqrt{z(z-2i)}|$. The same bound applies to $|\sin(\eta_0 \sqrt{z(z-2i)})|$, and analogous bounds apply to the other sine and cosine terms in (26). Applying the above inequalities to f defined by (25), it follows that

$$|f(z)| \le 6 e^{\eta_+ p(z)}, \quad (47)$$

for $z \ge 0$ and $|\beta| \le 1$, with

$$p(z) = |\mathrm{Im}\,\sqrt{z(z-2i)}| = \left\{ \frac{2z}{z + \sqrt{z^2+4}} \right\}^{1/2} \le \min(1, z^{1/2}).$$

Thus, for $t > 0$,

$$|f(t/\xi_N) t^{-1/2} e^{-t}| \le 6 t^{-1/2} \exp(\eta_+ \min(1, \sqrt{t/\xi_N}) - t).$$

If ξ_N is chosen such that $\xi_N \ge \eta_+^2/x_{m,n}$, it then follows that

$$|f(t/\xi_N) t^{-1/2} e^{-t}| \le 6 x_{m,n}^{-1/2} \exp(\eta_+ \min(1, \sqrt{x_{m,n}/\xi_N}) - x_{m,n}), \quad (48)$$

for $t \ge x_{m,n}$.

In the numerical results the values

K. V. Horoshenkov and S. N. Chandler-Wilde: Waveguide Green's functions

$$n = 40, \quad m = 22, \tag{49}$$

are chosen, for which $x_{m,n} = 30.26$. Then the criterion (48) ensures that

$$|f(t/\xi_N)t^{-1/2}e^{-t}| \leq 10^{-9},$$

for $t \geq x_{m,n}$, provided $\eta_+ \leq 9.4$ or

$$\xi_N \geq 0.34\eta_+^2. \tag{50}$$

The other contribution to the error, $|J - J_{m,n}|$, is that inherent in the Gauss–Laguerre quadrature formula. In the case $y = y_0 = 0$, when $\eta = \eta_0 = \eta_+ = 0$, provided the criterion (41) is satisfied so that the integrand is analytic within at least distance 0.75 of the positive real axis, it is not difficult to apply Ref. 16, Theorem 3(i), to show that the error in the n-point Gauss–Laguerre rule, $|J - J_{n,n}|$, tends to zero as $n \to \infty$, uniformly with respect to N and β, for $|\beta| \leq C$, where $C > 0$ is a positive constant. As remarked above, we adopt the values of n and m given by (49), whose values proved accurate in Ref. 16 for very similar integrands.

When $\eta_+ > 0$, the integrand has additional oscillatory terms: a typical such term is $\sin(\eta_+ \sqrt{z(z-2i)})$, the oscillatory behavior of which is determined, for $z \geq 0$, by

$$q(z) := \mathrm{Re}\,\sqrt{(z(z-2i))} = z^{1/2}\sqrt{\frac{z + \sqrt{z^2+4}}{2}}.$$

As η_+ increases the integrand becomes more oscillatory and a greater density of quadrature points is needed to sample this oscillation. A heuristic criterion for the choice of N is to insist that ξ_N be chosen large enough so that the Nyquist sampling criterion is amply satisfied in an average sense. The abscissae, sampling the integrand in (42), are distributed on the interval $[0, x_{m,n}/\xi_N]$ and the number of oscillations in this interval is $\eta_+ q(x_{m,n}/\xi_N)/(2\pi)$. Choosing ξ_N so that there are, on average, at least 11 integration points per oscillation leads to the heuristic criterion for the choice of ξ_N that

$$\tilde{c}q(x_{m,n}/\xi_N) \leq 1, \tag{51}$$

where $\tilde{c} = 11\eta_+/(2\pi m)$. Now, for $z \geq 0$,

$$z^{1/2}\max(1, z^{1/2}) \leq q(z) \leq \tilde{q}(z) \leq 1.5z^{1/2}\max(1, z^{1/2}),$$

where $\tilde{q}(z) := z^{1/2}(z^2+4)^{1/4}$. Thus a simpler and only slightly stricter criterion is obtained by replacing the function q by $\tilde{q}$ in (51). This slightly stricter criterion holds if and only if

$$\xi_N \geq \xi^* := x_{m,n}\tilde{c}\sqrt{2\tilde{c}^2 + \sqrt{1 + 4\tilde{c}^4}}. \tag{52}$$

Clearly $\xi^* > 2x_{m,n}\tilde{c}^2$. With the values of n and m proposed in Eq. (49), $x_{m,n} = 30.26$ so that $\xi^* > 2x_{m,n}\tilde{c}^2 = 0.38\eta_+^2$. Thus (50) is satisfied if (52) holds. Therefore, for the values $n = 40$ and $m = 22$ suggested, the various proposed criteria for the choice of N, Eqs. (41), (50), and (52), are all satisfied by choosing

$$N \geq 1 + \frac{1}{2H}\max(1, \xi^*) - \frac{\xi_0 - \xi}{2H}. \tag{53}$$

IV. THE PERIODIC AND CANYON GREEN'S FUNCTIONS

The previous section details formulas and a numerical scheme for computing the field due to the infinite array of sources (18). As discussed in the Introduction, it is much more frequently of interest to be able to compute the field due to an array of sources extending to infinity in both directions, that is, to be able to compute the function

$$G_\beta^{DP}(\mathbf{r}, \mathbf{r}_0; \alpha) = \sum_{l=-\infty}^{\infty} e^{-2il\alpha H} G_\beta(\mathbf{r}, \mathbf{r}_l). \tag{54}$$

Of course, the summation (54) can be written as two sums of the form (18). Precisely, let $\tilde{x}_l := 2x - x_{-l}$ and $\tilde{\mathbf{r}}_l := (\tilde{x}_l, y_0) = (2x - x_{-l}, y_0)$, for $l = 0, 1, \ldots$, so that $\tilde{\mathbf{r}}_l$ is the reflection of $\mathbf{r}_{-l}$ in the vertical line through $\mathbf{r}$. Then

$$G_\beta^{DP}(\mathbf{r}, \mathbf{r}_0; \alpha) = -G_\beta(\mathbf{r}, \mathbf{r}_0) + \sum_{l=0}^{\infty} e^{-2il\alpha H} G_\beta(\mathbf{r}, \mathbf{r}_l)$$

$$+ \sum_{l=0}^{\infty} e^{2il\alpha H} G_\beta(\mathbf{r}, \tilde{\mathbf{r}}_l)$$

$$= -G_\beta(\mathbf{r}, \mathbf{r}_0) + G_\beta^P(\mathbf{r}, \mathbf{r}_0; \alpha) + G_\beta^P(\mathbf{r}, \tilde{\mathbf{r}}_0; -\alpha). \tag{55}$$

Without loss of generality it will be supposed in the remainder of this section that $\mathbf{r}_0$ is the closest of the sources $\mathbf{r}_l$, $l = 0, \pm 1, \ldots$, to $\mathbf{r}$, so that

$$|\xi - \xi_0| \leq H. \tag{56}$$

Then $x_1 > x$ and $\tilde{x}_1 > x$, so that, for $N = 1, 2, \ldots$, $G_\beta^P(\mathbf{r}, \mathbf{r}_0; \alpha)$ and $G_\beta^P(\mathbf{r}, \tilde{\mathbf{r}}_0; -\alpha)$ have the representations given by (23) and (24). The calculation of the integral (24) in the four different cases, using Gauss–Laguerre quadrature, has been discussed in the last two subsections. [Of course, for the computation of $G_\beta^P(\mathbf{r}, \tilde{\mathbf{r}}_0; -\alpha)$, ξ_N must be replaced with $\tilde{\xi}_N := k(\tilde{x}_N - x) = \xi - \xi_0 + 2HN$ and α with $-\alpha$.] Given that (56) holds, the criterion (53) proposed for the choice of N is satisfied for the computation of both $G_\beta^P(\mathbf{r}, \mathbf{r}_0; \alpha)$ and $G_\beta^P(\mathbf{r}, \tilde{\mathbf{r}}_0; -\alpha)$ if N is chosen so that

$$N \geq 1.5 + \frac{1}{2H}\max(1, \xi^*). \tag{57}$$

The function $G^{DP}(\mathbf{r}, \mathbf{r}_0; \alpha)$ may be termed the *periodic impedance Green's function* for the Helmholtz equation in the upper half-plane, since it satisfies the impedance boundary condition on the ground surface and, clearly, has the periodicity property that

$$G^{DP}(\mathbf{r} + 2h\mathbf{i}, \mathbf{r}_0; \alpha) = e^{-2i\alpha H} G^{DP}(\mathbf{r}, \mathbf{r}_0; \alpha),$$

where $\mathbf{i}$ is a unit vector in the x direction. The periodic Green's function, $G^{DP}(\mathbf{r}, \mathbf{r}_0; \alpha)$, has applications in its own right, notably to problems of plane wave scattering by periodic structures (in which application α is the sine of the angle of incidence), but can also be used to construct solutions to problems of sound propagation in waveguides.

Consider the sound field generated by a point source of sound at $\mathbf{r}_0$ in the canyon formed by two parallel vertical rigid walls emerging from an impedance ground surface.
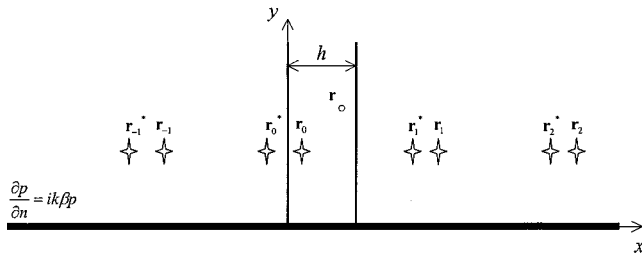
FIG. 4. The 2-D canyon/waveguide, showing the source and its images in the vertical walls.

Clearly (see Fig. 4), the problem can be solved by computing the positions of the infinite array of image sources formed by reflection in the rigid walls. It can be seen in Fig. 4 that these images form two doubly infinite periodic arrays, so that the effect of the rigid walls is to introduce additional sources at $\mathbf{r}_l$, $l = \pm 1, \pm 2, \ldots$, and at $\mathbf{r}_l^*$, for $l = 0, \pm 1, \pm 2, \ldots$, where $\mathbf{r}_l^* = \mathbf{r}_0^* + 2hl\mathbf{i}$ and $\mathbf{r}_0^*$ is the image of $\mathbf{r}_0$ in the wall at $x = 0$, i.e., $\mathbf{r}_0^* = (-x_0, y_0)$. Thus the solution to this problem of noise propagation in a canyon can be given in terms of the periodic Green's function, $G_\beta^{DP}(\mathbf{r}, \mathbf{r}_0; \alpha)$, with $\alpha = 0$, as

$$G_\beta^{can}(\mathbf{r}, \mathbf{r}_0) = G_\beta^{DP}(\mathbf{r}, \mathbf{r}_0; 0) + G_\beta^{DP}(\mathbf{r}, \mathbf{r}_0^*; 0). \quad (58)$$

In the case where the vertical walls are sound soft (i.e., the sound field vanishes on the vertical surfaces), the solution can be given in terms of the periodic Green's function, G_β^{DP}, as

$$G_\beta^{DP}(\mathbf{r}, \mathbf{r}_0; 0) - G_\beta^{DP}(\mathbf{r}, \mathbf{r}_0^*; 0),$$

and, in the case when one wall is rigid (that at $x = 0$) and the other sound soft, the solution is

$$G_\beta^{DP}(\mathbf{r}, \mathbf{r}_0; \pi/(2H)) - G_\beta^{DP}(\mathbf{r}, \mathbf{r}_0^*; \pi/(2H)).$$

To sum up, to compute the solution, $G_\beta^{can}(\mathbf{r}, \mathbf{r}_0)$, to the canyon problem, the Green's function is expressed in terms of the periodic Green's function via Eq. (58). The periodic Green's function is, in turn, expressed in terms of G_β^P through Eq. (55). Provided (56) holds, the terms $G_\beta^P(\mathbf{r}, \mathbf{r}_0; \alpha)$ and $G_\beta^P(\mathbf{r}, \tilde{\mathbf{r}}_0; -\alpha)$ in (55) can be calculated using Eqs. (23) and (24), with the Green's function G_β in (23) calculated using the method of Ref. 16. The calculation of the integral (24) is carried out via four different representations, discussed in Sec. III A. Specifically, it has been proposed that the representations (42)–(45) be used in the four different cases, with the integrals in these formulas evaluated using the Gauss–Laguerre quadrature rule (46), with n and m given by (49), and the parameter N chosen to be the smallest positive integer satisfying (57).

V. NUMERICAL RESULTS

Results are presented first of all illustrating the effect of the choice of N, the number of source contributions to be evaluated explicitly in Eq. (20), on the accuracy of the calculations. The field $G_\beta^P(\mathbf{r}, \mathbf{r}_0; \alpha)$ due to an infinite array of sources is evaluated using Eq. (23), with the integral I evaluated using Eqs. (42)–(45), the evaluation carried out as proposed in Sec. III B by the numerical integration formula (46) with the choices (49) for m and n. Results are shown for the case $\alpha = 0$. Plotted in Fig. 5 is ΔG_β^P, the absolute value of the difference between two calculations of $G_\beta^P(\mathbf{r}, \mathbf{r}_0; \alpha)$ using different values for N ($N = N_1$ and $N = N_2$). Having in mind applications in outdoor sound propagation, the surface impedance β is chosen to be that appropriate to a rigidly backed 100-mm layer of porous road surface. The acoustical properties of the porous layer as a function of frequency are calculated using the Attenborough model.[24,25] This model speci-
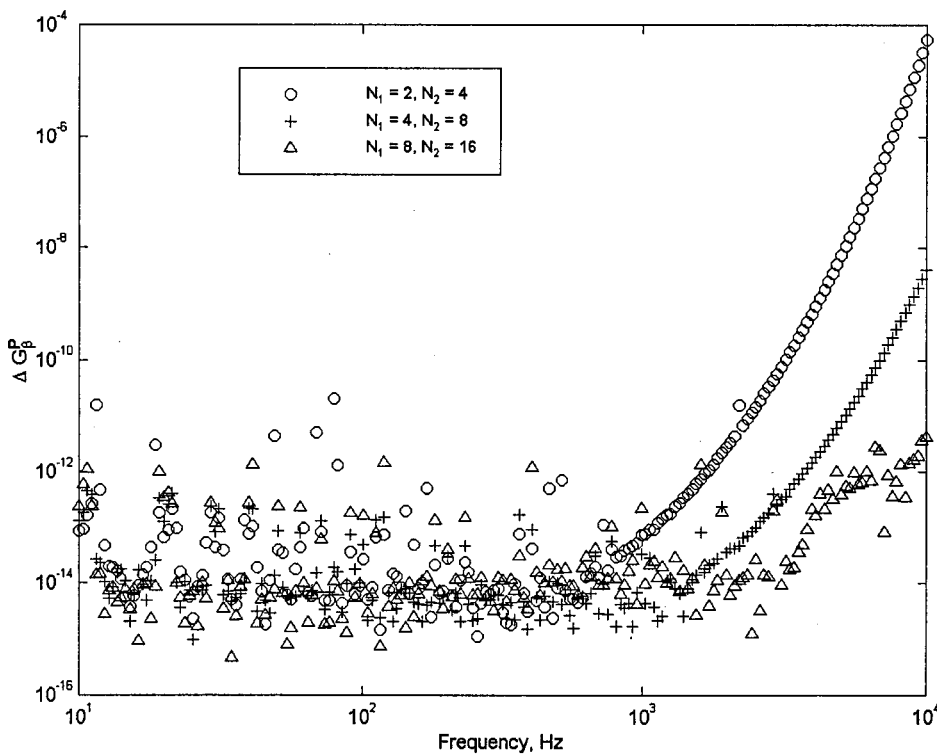

FIG. 5. Absolute error as a function of the parameter N calculated for sound propagation above 100-mm layer of porous road surface.

TABLE I. Values of the nonacoustic parameters used in the calculations.

Material	Flow resistivity, R_b (Pa s m^{-2})	Porosity, Ω	Tortuosity, q^2	Shape factor, s_p	Thickness, d (m)
Reflective ground	2×10^7	0.1	1.06	0.5	0.1
Porous road surface	3500	0.335	1.91	0.21	0.1
Highly absorbing ground	2×10^4	0.9	1.06	0.5	0.1

fies the acoustical admittance (β_b) and wave number (k_b) of the porous layer in terms of its porosity (Ω), tortuosity (q^2), flow resistivity (R_b), and a pore shape factor (s_p), giving[25]

$$\beta_b = \frac{\Omega}{q} g_\beta(\sqrt{-i}\lambda_A), \quad k_b = qk g_\beta(\sqrt{-i}\lambda_A),$$

where $\lambda_A = (1/2s_p)(8\rho_0 q^2 \omega/\Omega\sigma)^{1/2}$ and ρ_0 is the air density. The functions g_β and g_k are defined by $g_\beta(z) := \sqrt{g_c(z)/g_\rho(z)}$ and $g_k(z) := \sqrt{g_c(z)g_\rho(z)}$, in terms of the auxiliary functions $g_\rho(z) := [1-S(z)]^{-1}$ and $g_C(z) := 1 + (\gamma - 1)S(N_{\mathrm{Pr}}^{1/2}z)$. In these last expressions $\gamma = 1.4$ is the ratio of specific heats and $N_{\mathrm{Pr}} = 0.708$ is the Prandtl number, while S is the function defined by

$$S(z) := \frac{2J_1(iz)}{izJ_0(iz)} = \frac{2I_1(z)}{zI_0(z)},$$

with J_n the Bessel function of order n and I_n the corresponding modified Bessel function. In terms of β_b and k_b the impedance of the layer is

$$\beta = \beta_b \tanh(-ik_b d),$$

and the values of the nonacoustical parameters for the porous road surface are given in Table I. The positions of the source and the receiver were chosen to be $x_0 = 5.75$ m, $y_0 = 2.0$ m, $x = 1.5$ m, and $y = 1.5$ m. The value of h was set to 17 m, so that there is a spacing of 34 m between adjacent sources.

The error in Fig. 5 is mainly confined to the range $10^{-14} < \Delta G_\beta^P < 10^{-12}$, but increases at high frequency where $\eta_+ = k(y+y_0)$ is large ($\eta_+ \approx 640$ at 10 000 Hz). Results accurate to 10^{-12} are obtained at almost all frequencies up to 2000 Hz with $N = 2$, at frequencies up to 5000 Hz with $N = 4$, and across the frequency range with $N = 8$. At the highest frequency each doubling of N reduces the error by a factor of about 1000. The criterion proposed to ensure high accuracy, (20), suggests that N should increase approximately in proportion to $\eta_+^2/H = k(y+y_0)^2/h$. Specifically it recommends, for this geometry, $N \geq 5.9$ at 2000 Hz, $N \geq 13.5$ at 5000 Hz, and $N \geq 26.2$ at 10000 Hz.

The remaining figures show calculations of the canyon/waveguide Green's function $G_\beta^{can}(\mathbf{r},\mathbf{r}_0)$. A method for computing G_β^{can} efficiently has been proposed in Sec. IV. An alternative expression for G_β^{can} can be obtained as a normal mode decomposition (NMD),[26,27] namely,

$$G_\beta^{can}(\mathbf{r},\mathbf{r}_0) = \frac{1}{2iH}\sum_{n=0}^{\infty}\frac{\chi_n}{\zeta_n}\cos(k_n x_0)\cos(k_n x)$$
$$\times[e^{ik\zeta_n|y-y_0|} + R_n e^{ik\zeta_n(y+y_0)}], \quad (59)$$

where $\chi_n = 1$ when $n = 0$, $\chi_n = 2$ for all other values of n, $k_n = n\pi/h$, and $\zeta_n = \sqrt{1-k_n^2/k^2}$, with Im $\zeta_n > 0$ for $k_n > k$. In Eq. (59) R_n is the reflection coefficient for mode n from the impedance ground, given by

$$R_n = \frac{\zeta_n - \beta}{\zeta_n + \beta}. \quad (60)$$

Values of $G_\beta^{can}(\mathbf{r},\mathbf{r}_0)$ calculated using the method described in Sec. IV, with n and m given by (49), and N selected according to the criterion (57), are compared in Figs. 6–8 with the predictions of normal mode decomposition calculations, using the first 2000 terms in (59). Precisely, what is plotted in these figures is a sound pressure level given by

$$L = 20\log_{10}(\sqrt{k}|G_\beta^{can}(\mathbf{r},\mathbf{r}_0)|). \quad (61)$$

(The factor $\sqrt{k}$ ensures that the sound pressure level close to the source is approximately constant across the frequency range.) The three figures show predictions for different ground types (and so different variations of β with frequency), namely a reflecting boundary, a porous road surface, and a highly absorbing ground, with parameter values as shown in Table I. The positions of the source and the receiver were chosen to be $x_0 = 5.75$ m, $y_0 = 2.0$ m, $x = 1.5$ m and $y = 1.5$ m and the width of the canyon was set to $h = 17$ m. Figures 6–8 demonstrate excellent agreement between the results of the two methods throughout the spectral range considered.

Regarding the relative computational efficiency of the two methods the following comments can be made. In Sec. IV a specific quadrature rule for numerical integration has been suggested, with $m = 22$ (m is the number of evaluations of the integrand required). With m fixed the cost of the calculation method depends only on N, the number of source contributions calculated explicitly. The criterion (57), for selecting N to ensure a high accuracy, forces N to increase approximately in proportion to $\eta_+^2/H = k(y+y_0)^2/h$, although with a small constant of proportionality, and we have seen in Fig. 5 that with $N = 8$ very accurate results (error 10^{-12}) are obtained at even the highest frequency when $y + y_0 \approx 100$ wavelengths and $k(y+y_0)^2/h \approx 130$.

The representation (59) as a normal mode decomposition is to some extent complementary. For accurate results all the propagating modes (those for which $k_n \leq 1$) and at least some of the evanescent modes ($k_n > 1$) must be included in the summation. There are $\approx kh/\pi$ propagating modes so that this is the minimum number of mode contributions to be included, and so the cost is at least proportional to kh. In addition, when $k|y-y_0|$ is small the series converges slowly:

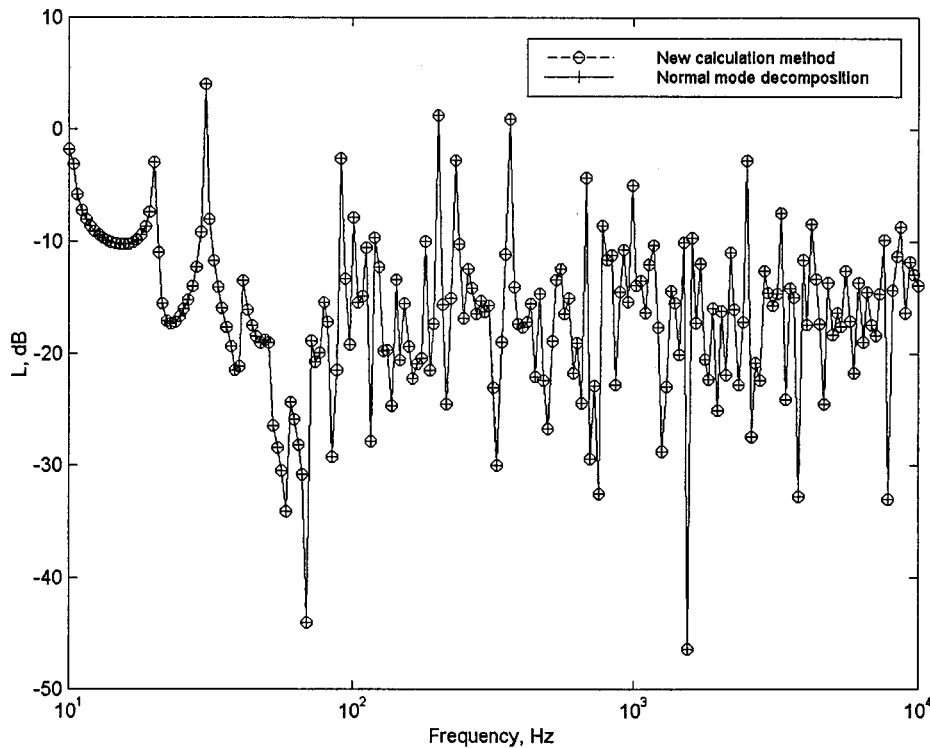K. V. Horoshenkov and S. N. Chandler-Wilde: Waveguide Green's functions

FIG. 6. Comparison of predictions using the method proposed in Sec. IV and the method of normal mode decomposition for sound propagation over reflective ground.

when $k|y-y_0|=0$ this convergence is very slow so that a very large number of evanescent modes need to be included in the summation, though this additional difficulty can be ameliorated by applying a Kummer's transformation[9] which accelerates the convergence of the series and reduces substantially the number of evanescent modes that need to be summed explicitly.[9,27]

The new representation proposed has a cost linearly dependent on N while the cost of evaluating the normal mode decomposition representation is proportional to the number of normal modes required for accurate results. Thus the new method will be faster when the ratio $N/($No. of normal modes required$)$ is small enough. In view of the above remarks, this ratio is $\leqslant C[k(y+y_0)^2/h]/[kh]=C[(y+y_0)/h]^2$, for some positive constant C, so that the new method of Sec. IV should be more effective for problems where h is large compared to $y+y_0$. To illustrate this, computational times required by the two methods are given in
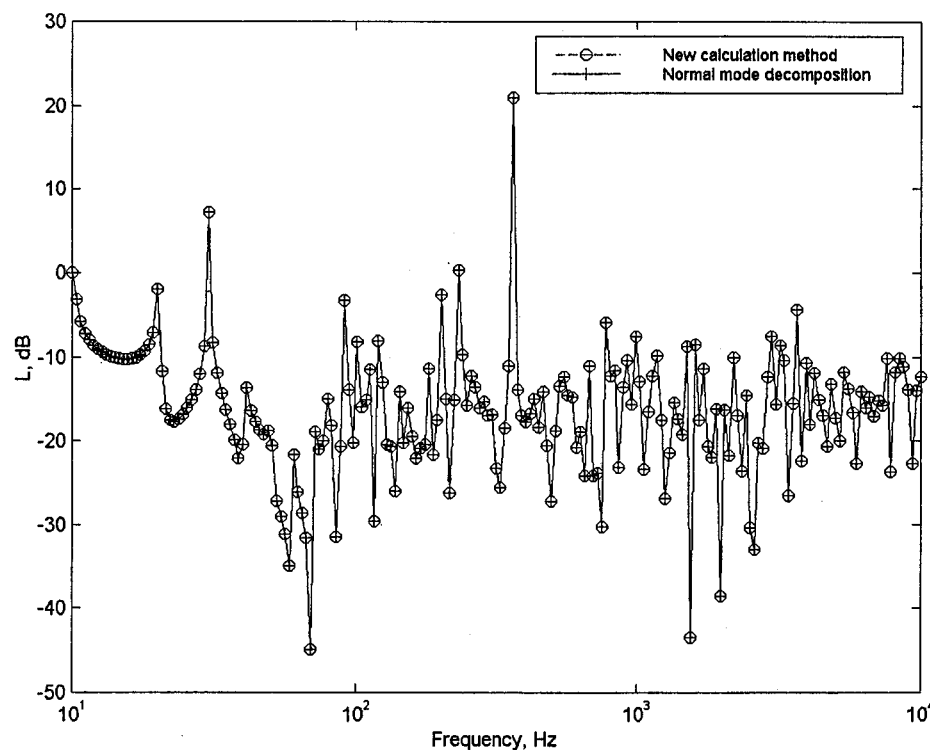

FIG. 7. Comparison of predictions using the method proposed in Sec. IV and the method of normal mode decomposition for sound propagation over a porous road surface.
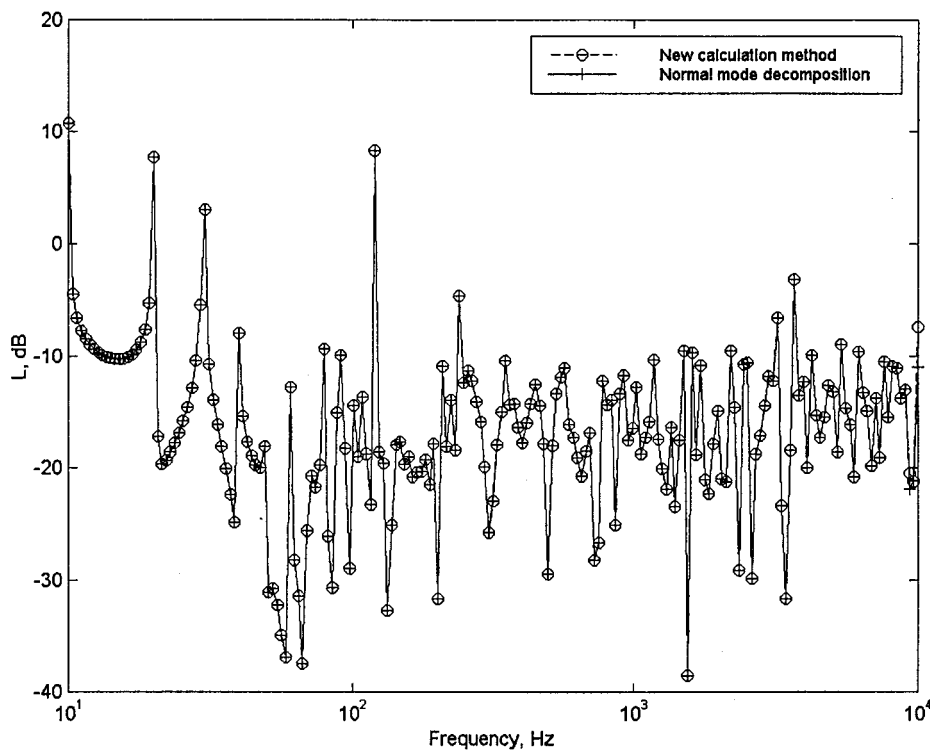
FIG. 8. Comparison of predictions using the method proposed in Sec. IV and the method of normal mode decomposition for sound propagation over a highly absorbing porous surface.

Table II. The CPU times tabulated are for the same geometry as for Fig. 5, i.e., $x_0 = 5.75$ m, $y_0 = 2.0$ m, $x = 1.5$ m, $y = 1.5$ m, and $h = 17$ m. As indicated above, the normal mode decomposition requires calculation of all the propagating modes and at least some of the evanescent modes for accurate calculations, how many depending on the size of $k|y - y_0|$ and on the acceleration procedure used. The third column shows CPU times for normal mode decomposition calculations using the same number of evanescent as propagating modes, so that approximately $2kh/\pi$ modes are computed and thus the CPU time increases approximately linearly with frequency. The remaining columns show the CPU times required for the method described in Sec. IV, with n and m given by (49). Specifically, the fourth column shows calculations with $N = 2$, which was found in Fig. 5 to give errors at most 10^{-12} for frequencies up to 2000 Hz, and the fifth column shows results with $N = 4$, which gave errors at most 10^{-12} up to 5000 Hz. It can be seen that, for this geometry, which has a small value of $[(y + y_0)/h]^2$ of approximately 0.04, and at higher frequencies where a large number

of modes is required, the new calculation method does indeed require less CPU time to compute accurate results.

VI. CONCLUSIONS

In this paper mathematical expressions for two-dimensional calculations of the sound field due to a mono-frequency point source in a canyon/waveguide have been derived, the canyon occupying the strip $0 < x < H$, $y > 0$ in the Oxy plane, and having rigid or sound soft walls at $x = 0$ and $x = H$ and an impedance boundary condition on $y = 0$. In the expressions proposed for this Green's function, and for the related periodic Green's function, the infinite sums of source contributions due to the multiple reflections from the walls are reduced to single integral terms. Further representations are proposed in which poles close to the integration path are removed and their contributions evaluated analytically, which greatly improves the accuracy of numerical integration. The error in numerical integration has been examined carefully, a specfic 22-point quadrature rule has

TABLE II. CPU times for the canyon problem of Fig. 5, with $x_0 = 5.75$ m, $y_0 = 2.0$ m, $x = 1.5$ m, $y = 1.5$ m, $h = 17$ m, and a 100-mm layer of porous road surface.

| Frequency (Hz) | Normal mode decomposition | | New calculation method | |
	No. modes	CPU time (ms)	$N = 2$ CPU time (ms)	$N = 4$ CPU time (ms)
125	25	1.46	2.93	3.91
250	50	1.95	2.83	3.91
500	100	2.68	2.92	3.91
1000	200	4.15	2.93	3.90
2000	400	6.83	2.93	3.90
4000	800	12.21	2.93	3.91
8000	1600	38.08	2.92	3.90

been proposed, and a criterion for selection of the parameter N (the number of source contributions to be treated explicitly) has been suggested. Numerical experiments show that, choosing N according to this criterion, the 22-point quadrature rule proposed gives extremely accurate results. The calculation procedure to be followed is summarized at the end of Sec. IV.

The numerical results include comparisons with an alternative representation of the function via normal mode decomposition. The new calculation procedure proposed complements this representation which becomes expensive to compute when kh is large (k the wave number and h the width of the waveguide) and/or when $k|y-y_0|$ is small ($|y-y_0|$ the difference in heights of source and receiver). By contrast, since the cost of the new method depends mainly on N which increases in proportion to $k(y+y_0)^2/h$, the new representations proposed are computationally efficient as long as $k(y+y_0)^2/h$ is not too large. The results presented show that very small absolute errors (10^{-12}) are obtained with $k(y+y_0)^2/h$ as large as 130 with $N=8$.

As discussed in the Introduction, it is expected that these new representations for the canyon/waveguide Green's function and the related periodic Green's function will prove useful in boundary element modeling of sound propagation in city streets and in waveguides, and for problems of scattering by periodic structures. For all these boundary element applications very efficient calculation procedures for the Green's function are crucial.

ACKNOWLEDGMENTS

[1] D. C. Hothersall, S. N. Chandler-Wilde, and M. N. Hajmirzae, "Efficiency of single noise barriers," J. Sound Vib. **146**, 303–322 (1991).

[2] D. Duhamel, "Efficient calculation of the 3-dimensional sound pressure field around a noise barrier," J. Sound Vib. **197**, 547–571 (1996).

[3] S. N. Chandler-Wilde, "Tyndall medal lecture: The boundary element method in outdoor noise propagation," Proc. Inst. Acoust. **19**(8), 27–50 (1997).

[4] D. C. Hothersall, K. V. Horoshenkov, and S. E. Mercy, "Numerical modelling of the sound field near a tall building with balconies near a road," J. Sound Vib. **198**, 507–515 (1996).

[5] K. V. Horoshenkov, D. C. Hothersall, and S. E. Mercy, "Scale modelling of sound propagation in a city street canyon," J. Sound Vib. **223**, 795–819 (1999).

[6] J. Kang, "Sound propagation in street canyons: Comparison between diffusely and geometrically reflecting boundaries," J. Acoust. Soc. Am. **107**, 1394–1404 (2000).

[7] E. Walerian, R. Janczur, and M. Czechowicz, "Sound level forecasting for city-centres. part 1: sound level due to a road within an urban canyon," Appl. Acoust. **62**, 359–380 (2001).

[8] S. H. Tang and K. M. Li, "The prediction of facade effects from a point source above an impedance ground," J. Acoust. Soc. Am. **110**, 278–288 (2001).

[9] C. M. Linton, "The Green's function for the two-dimensional Helmholtz equation in periodic domains," J. Eng. Math. **33**, 377–402 (1998).

[10] S. N. Chandler-Wilde, C. R. Ross, and B. Zhang, "Scattering by infinite one-dimensional rough surfaces," Proc. R. Soc. London, Ser. A **455**, 3767–3787 (1999).

[11] A. Meier, T. Arens, S. N. Chandler-Wilde, and A. Kirsch, "A Nyström method for a class of integral equations on the real line with applications to scattering by diffraction gratings and rough surfaces," J. Integral Eq. Appl. **12**, 281–321 (2000).

[12] K. V. Horoshenkov, "Control of road traffic noise in city streets," Ph.D. thesis, School of Engineering, University of Bradford, 1996.

[13] M. E. Veysoglu, H. A. Yueh, R. T. Shin, and J. A. Kong, "Polarimetric passive remote sensing of periodic surfaces," J. Electromagn. Waves Appl. **5**, 267–280 (1991).

[14] A. W. Mathis and A. F. Pearson, "A comparison of acceleration procedures for the two-dimensional periodic Green's function," IEEE Trans. Microwave Theory Tech. **41**, 567–571 (1996).

[15] J. DeSanto, G. Erdmann, W. Hereman, and M. Misra, "Theoretical and computational aspects of scattering from rough surfaces: one-dimensional perfectly reflecting surfaces," Waves Random Media **8**, 385–414 (1998).

[16] S. N. Chandler-Wilde and D. C. Hothersall, "Efficient calculation of the Green function for acoustic propagation above a homogeneous impedance plane," J. Sound Vib. **180**, 705–724 (1995).

[17] T. Oberhettinger and L. Baddi, *Tables of Laplace Transforms* (Springer, Berlin, 1973).

[18] S. N. Chandler-Wilde and D. C. Hothersall, "A uniformly valid far field asymptotic expansion for the Green function for two-dimensional propagation above a homogeneous impedance plane," J. Sound Vib. **182**, 665–675 (1995).

[19] C. M. Bender and S. A. Orszag, *Advanced Mathematical Methods for Scientists and Engineers* (McGraw–Hill, Tokyo, 1978).

[20] P. Concus, D. Cassatt, G. Jaehnig, and E. Melby, "Tables for the evaluation of $\int_0^x x^\beta e^{-x} f(x)dx$, by Gauss-Laguerre quadrature," Math. Comput. **17**, 245–256 (1963).

[21] M. Abramowitz and I. Stegun, *Handbook of Mathematical Functions* (Dover, New York, 1964).

[22] *Document D01BBF NAGFLIB: 1594/0:Mk 7:Dec 78 in NAG FORTRAN Library Manual, Mark 9* (Numerical Algorithms Group Ltd., Oxford, 1981).

[23] S. N. Chandler-Wilde and D. C. Hothersall, "On the Green function for two-dimensional acoustic propagation above a homogeneous impedance plane," Research Report, Department of Civil Engineering, University of Bradford, November 1991.

[24] K. Attenborough, "Acoustical impedance models for outdoor ground surfaces," J. Sound Vib. **99**, 521–544 (1985).

[25] S. N. Chandler-Wilde and K. V. Horoshenkov, "Padé approximants for the acoustical characteristics of rigid frame porous media," J. Acoust. Soc. Am. **98**, 1119–1129 (1995).

[26] P. M. Morse and K. U. Ingard, *Theoretical Acoustics* (Princeton U.P., Princeton, NJ, 1986).

[27] P. M. Morse and H. Feshbach, *Methods of Theoretical Physics* (McGraw–Hill, Tokyo, 1953).